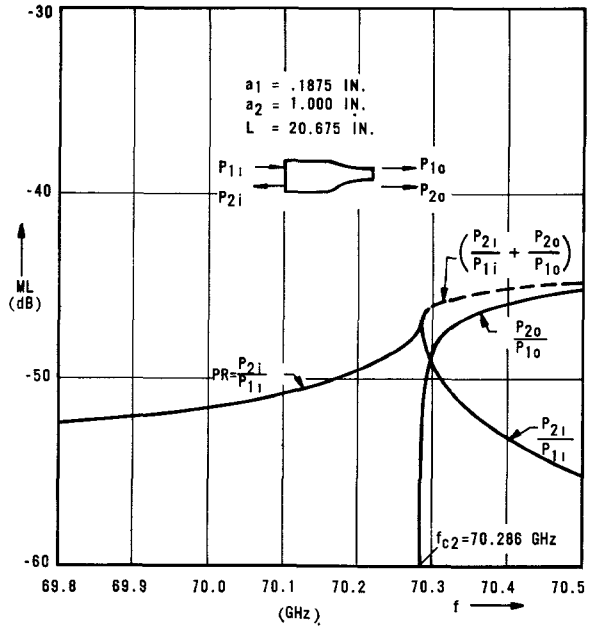

Fig. 11. Computed mode conversion of the 40-dB taper in the vicinity of the cutoff frequency of the H_{02} mode.

equations available, such an optimization has to be performed numerically. This is no trivial problem because of the severe constraint that, at least for manufacturing reasons, the slope should be continuous and monotonic. Nevertheless, with available computer programs for synthesis and analysis combined, the design of tapers for any mode discrimination and ratios a_2/a_1 can be accomplished in a short time if an interactive operating mode is possible.

Designed with this method, various 40-dB tapers having a small end diameter of 0.375 in and a large end diameter of 2.0 in were built. The H_{02} level found in a preliminary test agrees with the computed results and is below −40 dB. Moreover, it has been found that the mode conversion at cutoff of the spurious mode does not show any anomalies.

Acknowledgment

The authors wish to thank T. A. Abele, M. L. Liou, and H. C. Wang for their continuous support, as well as G. M. Blair and T. Kuliopulos for their efforts in manufacturing and finishing the tapers.

References

[1] R. W. Klopfenstein, "A transmission line taper of improved design," *Proc. IRE*, vol. 44, pp. 31–35, Jan. 1956.
[2] R. E. Collin, "The optimum tapered transmission line matching section," *Proc. IRE*, vol. 44, pp. 539–548, Apr. 1956.
[3] H. G. Unger, "Circular waveguide taper of improved design," *Bell Syst. Tech. J.*, vol. 37, pp. 899–912, 1958.
[4] S. E. Miller, "Waveguide as a communication medium," *Bell Syst. Tech. J.*, vol. 33, pp. 1209–1265, 1954.
[5] C. C. H. Tang, "Optimization of waveguide tapers capable of multimode propagation," *IRE Trans. Microwave Theory and Tech.*, vol. MTT-9, pp. 442–452, Sept. 1961.
[6] R. P. Hecken, "A near optimum matching section without discontinuities," *IEEE Trans. Microwave Theory and Tech.*, vol. MTT-20, pp. 734–739, Nov. 1972.
[7] M. A. Gerdine, Bell Laboratories, private communication.
[8] E. A. Marcatili and A. P. King, "Transmission loss due to resonance of loosely-coupled modes in a multi-mode system," *Bell Syst. Tech. J.*, vol. 35, pp. 899–906, 1956.
[9] C. C. H. Tang, "Forward and backward scattered modes in multimode nonuniform transitions," *IEEE Trans. Microwave Theory and Tech.*, vol. MTT-16, pp. 494–502, Aug. 1968.

Calculation of Inductance of Finite-Length Strips and its Variation with Frequency

A. GOPINATH AND P. SILVESTER

***Abstract*—The inductances of finite-length strips over a ground plane are calculated by the Galerkin method. The formulation is in terms of the quasi-static skin-effect equation. The numerical technique used is discussed and sample results are presented.**

Manuscript received August 18, 1972; revised January 21, 1972. This work was supported by the Communications Research Centre, Ottawa, and by the National Research Council of Canada. This work was performed while A. Gopinath was a Visiting Research Fellow at McGill University.

A. Gopinath was with McGill University, Montreal, Que., Canada. He is now with the School of Electronic Engineering Science, University College of North Wales, Bangor, Caerns, United Kingdom.

P. Silvester is with the Department of Electrical Engineering, McGill University, Montreal, Que., Canada.

I. Introduction

THE CALCULATION of inductance of finite-length conducting strips is currently of some interest. The strips concerned, for example, could take the form of interconnections between active and passive elements in integrated circuits or alternatively guiding structures such as microstrip lines in microwave integrated-circuit modules. In general, semiempirical formulas of Grover [1] are used, but these are not always satisfactory, nor are they comprehensive.

The capacitances associated with such structures have been calculated by several authors [2]–[4] and use, among

others, the moment method or a more generalized form of the Galerkin method [5]. These calculations are based on the assumption that the charge, a scalar quantity, is unknown and can be approximated by an expansion in a trial function set. Since the potential is known, the integral equation with the Green's function may then be used to solve the problem. The capacitance thus calculated is independent of frequency.

A similar technique, however, is not always applicable for the inductance calculation. The current distribution is a vector and a function of frequency. The inductance decreases to a limited extent with frequency, and any formulation should take account of this variation. While the specific case of high-frequency inductance is of interest to microwave engineers for microstrip lines, the present paper considers the more general formulation which evaluates inductance of strips at any frequency of interest.

The integro-differential equation based on skin effect is derived and the technique of numerical solution by the Galerkin method is discussed. In the course of this work a method for the choice of suitable basis functions, using the generalized matrix inversion concept, was developed, and this is also discussed briefly. A computer program was written for the calculation of inductance of finite-length strips over a ground plane and this corresponds to the case of microstrip lines. It is known that the presence of the dielectric substrate in these lines does not affect the longitudinal current distribution associated with the inductance [6], [7]. The paper concludes with some numerical examples of the inductance of finite-length strip lines over a ground plane.

II. Formulation of Problem

The problem is formulated in the orthodox quasi-static skin-effect form [8], and hence leads to estimates of inductance and inductance decrement with frequency. Retardation effects are neglected. A typical case considered is shown in Fig. 1, where w is the width of the strip and h the spacing to the ground plane.

In general, the magnetic vector potential is given by

$$A = \mu_0 \int G\bar{J}\, dV \tag{1}$$

where G is the Green's function and is given by

$$G = \frac{1}{4\pi\sqrt{(x-x_0)^2 + (y-y_0)^2 + (z-z_0)^2}}$$

for nonmagnetic substrates.

$\bar{J}$ is the current density distribution on the strip: the unknown time-varying quantity.

For magnetic substrates, the Green's function would require to take account of the images set up.

The electric field now is

$$\bar{E} = -\frac{\partial \bar{A}}{\partial t} - \nabla\phi \tag{2}$$

where ϕ is the impressed voltage on the strip which causes current to flow.

Also, from Ohm's law,

$$\bar{J} = \sigma\bar{E} \tag{3}$$

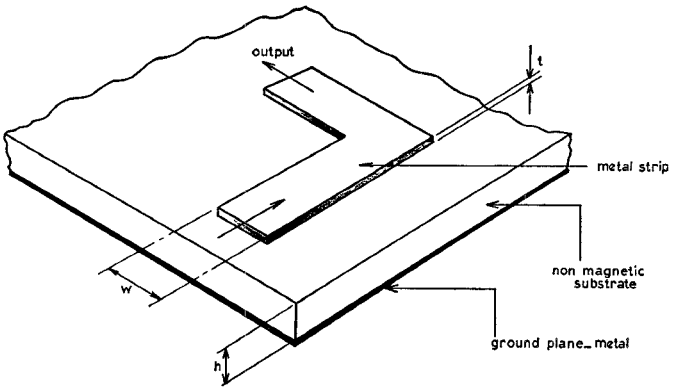

Fig. 1. Typical geometry of strip analyzed. w = width of strip; h = spacing to ground plane.

where σ is the strip conductivity. Substituting from (1) and (3), (2) becomes

$$\bar{J} + \mu\sigma \frac{\partial}{\partial t} \int G\bar{J}\, dV = -\sigma\nabla\phi. \tag{4}$$

This is the vector integro-differential skin-effect equation; its scalar component parts are all formally identical. The unknown current density distribution $\bar{J}$ is to be evaluated for a given geometry and excitation ϕ. When this is solved, the inductance may be calculated from the following relationships:

$$\int \bar{A}\cdot\bar{J}\, dV = LI^2 \tag{5}$$

$$\left[\int \bar{J}\, dV\right]^2 = I^2. \tag{6}$$

To solve (4), the homogeneous solutions for $\bar{J}$ with the right-hand side set to zero, an eigenvalue problem, are evaluated. Next, Laplace's equation is solved for ϕ over the strip or strips with the given terminal excitation, and subsequently the unknown coefficients associated with the eigenmodes of the homogeneous problem are evaluated for the given excitation ϕ, and hence known $\nabla\phi$. When the current distribution is known, it is a simple matter to evaluate the inductance.

III. Method of Numerical Solution

For convenience, the thickness of the strip t is assumed to be small compared with skin depth at the highest frequency of interest, and therefore variation of the current in the thickness may be neglected. The volume integrals hence become surface integrals, and the surface become line integrals. The notation of V and S is, however, retained. We also assume that the strips lie in the planes defined by z = constant, and therefore the current density $\bar{J}$ is now a two-component vector involving J_x and J_y only, related through the divergence equation

$$\frac{\partial J_x}{\partial x} + \frac{\partial J_y}{\partial y} = 0. \tag{7}$$

Note that the divergence equation neglects the charge term as only quasistatic conditions are considered. Further, the

current $\bar{J}$ should satisfy the boundary conditions, i.e., the normal componet of current must be zero at the strip edges.

Suppose a basis set of functions $\{\bar{\xi}_n\}$ is obtained such that each and every member satisfies (7) and the boundary conditions. The current $\bar{J}$ now may be approximated by $\bar{W}$ which is expanded in terms of this basis:

$$\bar{J} \simeq \bar{W} = \sum_{i=1}^{n} a_i \bar{\xi}_i \tag{8}$$

where a_i are the unknown coefficients. Note that each component of $\{\bar{\xi}_i\}$ is a vector representing J_x and J_y, and is a function of x and y.

The approximation $\bar{W}$ is substituted in the homogeneous equation obtained by setting the right-hand side of (4) to zero. Taking the scalar product of this equation with $\bar{\xi}_1$, $\bar{\xi}_2, \cdots, \bar{\xi}_n$ results in a set of equations of the form

$$\sum_{i=1}^{n} a_i \left(\int G\bar{\xi}_i \, dV, \bar{\xi}_k \right) = \lambda_j \sum_{i=1}^{n} a_i \langle \bar{\xi}_i, \bar{\xi}_k \rangle, \qquad k = 1, 2, \cdots, n \tag{9a}$$

where the scalar product is defined by

$$\langle \bar{X}, \bar{Y} \rangle = \int \bar{X} \cdot \bar{Y} \, dV. \tag{9b}$$

This is a homogeneous equation and when the integrals are evaluated results in a matrix eigenvalue of the form

$$P\boldsymbol{a} = \lambda Q\boldsymbol{a}. \tag{9c}$$

Both P and Q are symmetric positive-definite matrices. Numerical evaluation of the eigenvalues and vectors may then be performed by suitable algorithms.

Suppose the solution is given by

$$\bar{W} = \sum_{j=1}^{n} c_j \bar{\psi}_j \tag{10}$$

where

$\{\bar{\psi}_j\}$ eigenvector set;
$\{\lambda_j\}$ corresponding eigenvalue set;
c_j unknown coefficients associated with the $\bar{\psi}_j$.

Substituting (10) in (4) results in the following equation:

$$\sum_{j=1}^{n} (1 + j\omega\mu\sigma\lambda_j) c_j \bar{\psi}_j = -\sigma \nabla\phi. \tag{11}$$

The impressed voltage ϕ satisfies Laplace's equation:

$$\nabla^2\phi = 0$$

and hence is known for given terminal excitation.

To solve for c_j, the scalar product of (10) is taken with the eigenvectors ψ_j to give

$$\sum_{j=1}^{n} (1 + j\omega\sigma\mu\lambda_j) c_j \langle \bar{\psi}_j, \bar{\psi}_k \rangle = -\sigma \langle \nabla\phi, \bar{\psi}_k \rangle, \qquad k = 1, 2, \cdots, n.$$

However, the $\bar{\psi}_j$ form an orthogonal set, and hence

$$c_j = \frac{-\sigma \langle \nabla\phi, \psi_j \rangle}{(1 + j\omega\mu\sigma\lambda_j) \langle \psi_j, \psi_j \rangle}. \tag{12}$$

From this, the coefficients c_j, which are complex, may be evaluated, and therefore the current $\bar{J}$ is known. The stored energy and the inductance may be calculated from (5) and (6).

IV. Choice of Basis Function Set

The double volumetric integrals of (9) require to be performed over, say, L-shaped strips. One also has to contend with singularities as a result of the three-dimensional Green's function G. Spatial discretization of the strip or strips into rectangular elements facilitates the evaluation of the integrals and permits the elimination of the singularity [5]. Thus local basis functions for the current density are defined over each element (zero outside), and these have to satisfy the divergence condition and the element boundary conditions.

The procedure followed here is based on the general mathematical techniques published elsewhere [9], and the results are outlined briefly. Suppose over any element the current is expanded as

$$\bar{J} \simeq \bar{W} = \bar{a}_x J_x + \bar{a}_y J_y \tag{13}$$

where $\bar{a}_x$ and $\bar{a}_y$ are unit vectors in the x and y directions and

$$J_x = \sum_i p_i f_i(x, y)$$
$$J_y = \sum_i q_i f_i(x, y) \tag{14}$$

where $\{f_i\}$ is the set of bivariate polynomials: 1, x, y, x^2, xy, y^2, $\cdots$, etc., complete to degree, say, n_{deg}, and p_i and q_i are the unknown coefficients.

Substituting these expansions in the divergence equation (7) and equating coefficients of like polynomials, p_i and q_i are related. From this relationship, the current may now be expanded in terms of a modified basis $\{\bar{\xi}_i\}$; each $\bar{\xi}_i$ is a vector and satisfies the divergence condition. It can be shown that $\{\bar{\xi}_i\}$ is given by

	$\bar{\xi}_1$	$\bar{\xi}_2$	$\bar{\xi}_3$	$\bar{\xi}_4$	$\bar{\xi}_5$	$\bar{\xi}_6$	$\bar{\xi}_7$	$\bar{\xi}_8$	$\bar{\xi}_9$	
J_x	1	0	y	x	0	y^2	$2xy$	x^2	0,	etc.
J_y	0	-1	0	$-y$	$-x$	0	$-y^2$	$-2xy$	$-x^2$	

Therefore, the current may now be expanded as

$$\bar{J} \simeq \bar{W} = \sum_i b_i \bar{\xi}_i \tag{15}$$

where b_i are the unknown coefficients. Note that in satisfying the divergence equation, the number of unknowns per element has been reduced from $(n_{\text{deg}}+1)(n_{\text{deg}}+2)$ to $(n_{\text{deg}}+1)(n_{\text{deg}}+4)/2$.

It is now necessary to impose boundary conditions on this expansion of $\bar{J}$. Since local basis functions are used, inter-element conditions require continuity of both components of current, and at the strip edge the normal component is zero. At the inflow and outflow edges no conditions are imposed at this stage, as the necessary conditions are set by the right-hand side of (4) by $\nabla\phi$.

The continuity of current is rigidly enforced at the common boundaries. If the basis set has the highest degree given by n_{deg}, then $n_{\text{deg}}+1$ conditions specify the continuity of each component entirely on any one boundary. Thus for example, at the boundary between elements 1 and 2, the

continuity of J_x is ensured by

$$\langle R, (J_{x1} - J_{x2})\rangle = 0 \tag{16a}$$

where R is given by $1, x, \cdots, x^{n_{deg}}$ or by $1, y, \cdots, y^{n_{deg}}$, if the boundary is parallel to the x or y axis, respectively, and the scalar product is defined by

$$\langle A, B\rangle = \int_{l_1}^{l_2} A \cdot B \, dl. \tag{16b}$$

The matrix equation thus obtained for the common boundaries may be rectangular or, if square, may have a rank less than the number of unknowns. If, however, this is not the case, the existing degrees of freedom have all been utilized in satisfying these conditions, and therefore the problem requires a larger number of trial functions. Using the concept of weak generalized inverse (see the Appendix), a null vector set can be obtained from the matrix equation, which set now satisfies the common boundary conditions at the expense of a reduction of the degrees of freedom. This null vector set is now used as the new basis set for the expansion of $\bar{J}$.

The strip-edge boundary conditions are next imposed, i.e., the normal component of current is zero, or in general,

$$B\bar{J} = g. \tag{17}$$

This may be satisfied by minimizing the functional

$$F = \langle B\overline{W}, \overline{W}\rangle - 2\langle g, \overline{W}\rangle \tag{18}$$

where the inner product, defined in (16b), is carried out piecewise over the relevant boundaries and the minimization is over the unknown coefficients of the basis set.

Since the operator B is not necessarily positive definite, "minimization" of F by the usual method, i.e., setting $\partial F/\partial s_i = 0$, S_i are the unknown coefficients, will give a matrix equation, the solution of which will not necessarily satisfy boundary conditions. It then becomes necessary to examine the diagonal of the matrix generated by the minimization procedure and to eliminate those equations which do not produce a true minimum, i.e., diagonal terms with zero or negative values. An alternative is to specify a least-squares fit which does not suffer from this difficulty. This takes the form of minimizing

$$\eta = \|B\overline{W} - g\|, \qquad \text{on an } L_2 \text{ norm.} \tag{19}$$

For the currents at the strip edge, g is zero, the least-squares minimization is easily imposed, and the null vector set obtained as a solution of the resulting matrix equation satisfies the edge conditions. Thus if the vector set which satisfies common boundaries is used here, the new null set satisfies both conditions, and also the divergence condition, and forms the basis $\{\bar{\xi}_i\}$.

The formulation of the problem in the above form and its subsequent numerical solution has the limitation that it requires all the strip elements to be rectangles, and preferably with sides parallel to the axes. As the method stands, it is also not possible to evaluate the inductance of lengths of strips connected to semi-infinite lines. However, it is expected that this last limitation can be removed by the use of basis functions defined on a semi-infinite strip and corresponding modifications to the computer program.

V. Numerical Implementation and Results

A computer program for the calculation of the inductance of finite-length strip lines over a ground plane has been written, and results obtained for two different geometries are presented here.

A. Computational Sequence in the Calculation

The geometry of the problem and associated discretization of the strips into rectangular elements, together with the degree of polynomial of expansion functions, form the input data to the computer program. The calculation of the inductance may be divided into three parts: the solution of the eigenproblem of (9), the solution of Laplace's equation for the impressed potential ϕ, and, finally, the calculation of the current distribution for the particular frequency, from (12), and the estimation of inductance of the structure based on (5) and (6). The computer program follows this sequence of calculation.

The unknown current distribution is expanded in the polynomial set of (15) and the interelement boundary conditions, continuity of J_x and J_y, are rigidly enforced by means of equations of the form of (16) to give a matrix equation. Using the generalized matrix inverse (see the Appendix), the null set extracted from this matrix equation now is a combination of the original basis set, which satisfies the interelement conditions. This null set is used as an expansion basis to satisfy the homogeneous boundary conditions at the edge by means of (19). Computationally, it is convenient to use the original basis set in the homogeneous equation to setup the matrix, and then post and premultiply the matrix thus obtained by the null set and its transpose, respectively. The null set extracted from this final matrix equation now satisfies all boundary conditions. The inner-product line integrals in these equations are evaluated by Gaussian quadrature, with an adequate number of points. The null set finally obtained above is used in the eigenproblem of (9), and, here also, the original basis evaluates the matrices and subsequently these are post and premultiplied by the null set to give the matrix equation (9c). The integrals of (9) are also evaluated by Gaussian quadrature in two dimensions, and the singularity due to the Green's function is eliminated by the technique described elsewhere [5]. The evaluation of the eigenvalues and vectors of (9c) is by standard subroutines: reduction of Q by Choleski decomposition to LL^T, and the pre and post-multiplication of P by L^{-1} and $(L^T)^{-1}$, respectively; the Householder tridiagonalization of $L^{-1}PL^{-T}$, and the evaluation of the eigenvalues by bisection using the Sturm sequence; and, finally, the evaluation of the eigenvectors by iteration in the tridiagonal matrix and their subsequent inverse Householder transformation and restoration to the original matrix. The eigenvalues and vectors thus obtained are stored.

The Laplace equation is next solved, discretized with the same number of rectangular elements as above. Here, ϕ is approximated in an expansion in the bivariate polynomial set of (14) of degree one greater than used in the eigenproblem in the expansion of the approximation for $\bar{J}$, as $\nabla\Phi$ is then in the same vector space as the approximation for $\bar{J}$. The interelement boundary conditions are first specified (continuity of Φ, and its normal derivative) and then the homogeneous conditions (the Neumann condition $\partial\phi/\partial n$) at the strip edge and the end conditions are next imposed. The end conditions determine the inflow and outflow of the current, and thus are governed by geometry of the problem, but within these constraints may be arbitrary. The null set thus obtained is used as the basis for Φ in the minimization of the functional

$$F_L = \langle \nabla\Phi, \nabla\Phi\rangle$$

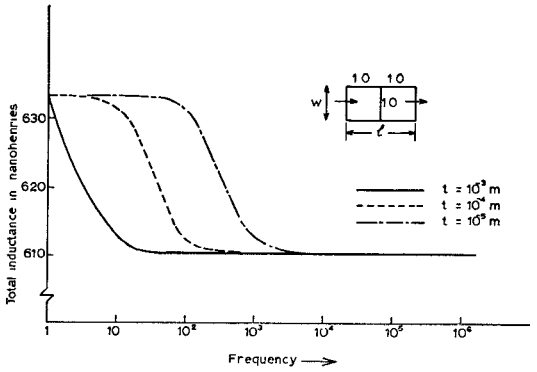

Fig. 2. Variation of inductance with frequency for a straight strip of length 2.0 m, $w = 1.0$ m, $w/h = 1.0$, ground plane h, $\rho = 1.721 \times 10^{-6}$ $\Omega \cdot$m, and $\sigma = t/\rho$. Division into two rectangles.

where the inner product is defined by (9b). Since the Neumann condition $\partial\Phi/\partial n$ is "natural" to this functional and automatically satisfied, this need not be imposed, nor is it necessary to impose the continuity of the normal derivative of Φ at the interelement boundary.

With the results of these two parts of the program available, the current distribution is evaluated through (12) at the frequency of interest, and the stored energy integral of (5) is also evaluated. Note that the matrix P in (9c) is the stored energy integral in this method, and using the new known coefficients (which will be complex, in general) of the current expansion set, the evaluation involves just two (complex) matrix multiplications (premultiply P by the conjugate coefficient vector and then postmultiply the resultant by the coefficient vector). The current I is then evaluated to give the inductance.

B. Examples

The first test problem considered a straight finite-length line over a ground plane of length 2.0 units (meters) for a width to height ratio (w/h) of 1.0. Fig. 2 shows the variation of inductance with frequency. Since the strip thickness is assumed to be small, the conductivity used is in mhos and equal to the ratio of thickness to resistivity in (4). Changing σ (or thickness) results in a frequency variation whose pattern remains the same, but starts at a different frequency position, and this is also illustrated in Fig. 2. Note that changing the conductivity does not change the dc or high-frequency value of inductance. These results were obtained with the line divided into two rectangles. Increasing the number of rectangles from two to four results in a very small change in the results, as shown in Table I. All these results were computed with polynomials up to quadratics using Gauss–Legendre three-point quadrature formulas for numerical integration.

Increasing the line length from 2 units to 16 units for $w/h = 1.0$ shows the asymptotic approach of the calculated high-frequency inductance to the infinite-length strip inductance in Fig. 3. It is noted that this is rather slow, but illustrates the physical behavior of the line. Other numerical results on strips of different w/h have also been obtained, and these will be discussed in Section V-C.

Calculations for a right-angle corner were also performed for three values of w/h with different length arms. These were obtained with a subdivision of the strip into eight rectangles using expansions up to quadratic polynomials. The variation

TABLE I

COMPARISON OF CALCULALED INDUCTANCE OF A STRAIGHT STRIP OVER GROUND PLANE DIVIDED INTO TWO AND FOUR RECTANGLES

Frequency in Hz	Inductance 2 rectangle subdivision	in nanohenries 4 rectangle subdivision
0.0	633.24	636.64
1.0	633.24	636.64
5.0	633.24	636.63
10	633.22	636.62
15	633.20	636.59
10^2	631.43	634.63
10^3	612.84	612.69
10^4	610.53	608.47
10^5	610.50	608.42

Note. $w/h = 1.0$; $w = 1$ m; length $= 2.0$ m; $\rho = 1.721 \times 10^{-6}$ $\Omega \cdot$m; strip thickness $t = 10^{-4}$ m; $\sigma = t/\rho$; ground-plane spacing $= h$.

of the inductance with frequency is also obtained and shown in Fig. 4 for $w/h = 1.0$ and each arm of length 2.0. Table II shows the variation of inductance with w/h and for two values of arm lengths.

The computer program is capable of evaluating arbitrary-shaped strips over a ground plane which can be subdivided into rectangles up to a maximum of ten rectangles with quadratic polynomials. The strips, however, require to lie in the $z =$ constant planes.

C. Comparison with Known Results

The inductance of finite straight lengths of a strip over a ground plane can be estimated from Grover [1]. Table III shows a comparison between our calculated dc values for a length 8 m long, $w = 1.0$ m, and three values of h: 2.0, 1.0, and 0.5 m, corresponding to w/h ratios of 0.5, 1.0, and 2.0, with those of Grover, and the discrepancy at worst is 1.8 percent. No published data exist for the inductance of strips in the form of L, but it is expected that the results are within 2-percent accuracy.

VI. CONCLUSIONS

An integro-differential skin-effect formulation was used to evaluate inductance of arbitrary-shaped finite-length conducting strips over a ground plane. The comparison between calculated and known results shows good agreement. The computer program written in Fortran is capable of handling up to a maximum of ten rectangular subdivisions with a quadratic expansion basis. Other geometries of strips over ground planes can also be examined with this program, provided only that the strip or strips lie in $z =$ constant planes and can be subdivided into rectangular elements.

APPENDIX

Let A be an $m \times n$ matrix of rank r. Gaussian elimination of the elements of A is carried out with interchanges for rows and columns as needed until only zero pivots remain. Then matrix equation becomes

$$AX = \begin{bmatrix} L_1 \\ L_2 \end{bmatrix} \begin{bmatrix} U_1 & U_2 \end{bmatrix} \begin{bmatrix} X_1 \\ X_2 \end{bmatrix} = \begin{bmatrix} f_1 \\ f_2 \end{bmatrix} = f. \qquad (20)$$

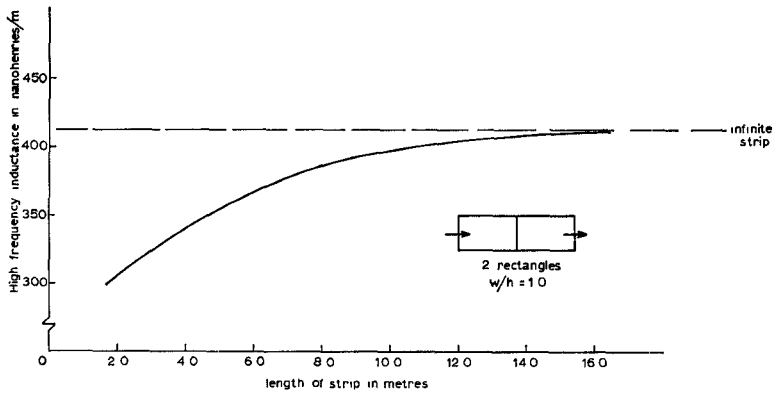

Fig. 3. High-frequency inductance per meter plotted against the total length of line showing asymptotic approach to the high-frequency inductance per meter of an infinite line. $w = 1.0$ m; $w/h = 1.0$; ground-plane spacing $= h$.

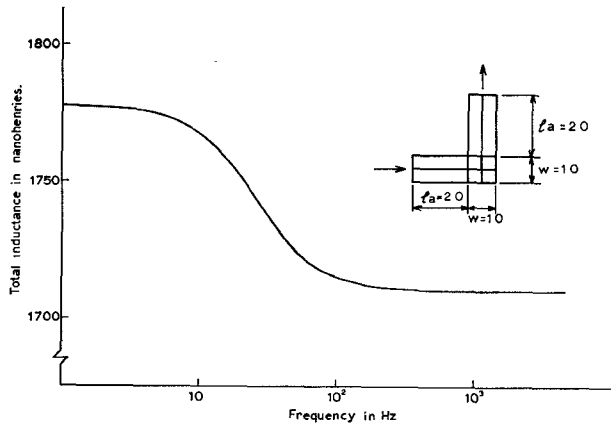

Fig. 4. Frequency variation of finite-length strip in the shape of an L (right-angle bend). $w = 1.0$; $w/h = 1.0$; length of arms $l_a = 2.0$ m. Subdivision into eight rectangles; expansion polynomials up to quadratics.

TABLE II

INDUCTANCE OF RIGHT-ANGLE BEND

w/h	ℓ_a in m	$L_{d.c.}$ in nH	$L_{h.f.}$ in nH
0.5	1.0	988.9	934.4
	2.0	2037.	1960.
1.0	1.0	887.7	842.6
	2.0	1778.	1710.
2.0	1.0	726.2	692.8
	2.0	1408.	1347.

Note: $w = 1.0$ m; length of arm $= l_a$; L_{de} is the total inductance at zero frequency value; L_{hf} is the high frequency; ground-plane spacing $= h$.

Hence,

$$X_1 = U_1^{-1}L_1^{-1}f_1 - U_1^{-1}U_2X_2$$

$$f_2 = L_2L_1^{-1}f_1. \tag{21}$$

Therefore,

$$X = A^+f + Nz \tag{22}$$

TABLE III

COMPARISON BETWEEN GROVER'S [1] DC INDUCTANCE ESTIMATE AND CALCULATED VALUES FOR A STRAIGHT FINITE-LENGTH STRIP $w = 1.0$ m OVER A GROUND-PLANE SPACING h

w/h	ℓ	Grover's result	Inductance in nano-Henries calculated by this method
1.0	2.0m	635.74 nH	636.6
1.0	8 m	3166.24	3211.
2.0	8 m	2319.52	2356.
0.5	8 m	3926.96	3969

where A^+ and N are the row–column reinterchanged forms:

$$A^+ = \begin{bmatrix} U_1^{-1}L_1^{-1} & 0 \\ 0 & 0 \end{bmatrix} \qquad N = \begin{bmatrix} -U_1^{-1}U_2 \\ I \end{bmatrix}$$

and $n-r$ components of z are arbitrary.

The columns of the matrix N form a basis in the null space of the matrix A, and matrix A^+ satisfies the equations

$$AA^+A = A$$

$$A^+AA^+ = A^+.$$

Hence, the first term of the right side of (22) specifies the inhomogeneous solution of (20), while the second term provides all possible homogeneous solutions.

ACKNOWLEDGMENT

The authors wish to thank P. Benedek and Z. Csendes, of McGill University, for the many discussions and helpful comments during the course of this work.

REFERENCES

[1] F. W. Grover, *Inductance Calculation: Working Formulas and Tables*. New York: Dover, 1946.
[2] P. D. Patel, "Calculation of capacitance coefficients for a system of irregular finite conductors on a dielectric sheet," *IEEE Trans. Microwave Theory Tech.*, vol. MTT-19, pp. 862–869, Nov. 1971.
[3] A. Farrar and A. T. Adams, "Computation of lumped microstrip capacities by matrix methods—Rectangular sections and end effect," *IEEE Trans. Microwave Theory Tech.* (Corresp.), vol. MTT-19, pp. 495–496, May 1971.
[4] ——, "Matrix methods for microstrip three-dimensional problems,"

IEEE Trans. Microwave Theory Tech., vol. MTT-20, pp. 497–504, Aug. 1972.
[5] P. Benedek and P. Silvester, "Capacitance of parallel rectangular plates separated by a dielectric sheet," *IEEE Trans. Microwave Theory Tech.*, vol. MTT-20, pp. 504–510, Aug. 1972.
[6] A. Gopinath, B. Easter, and R. Horton, "Microstrip loss calculations," *Electron. Lett.*, vol. 6, pp. 40–42, 1970.
[7] E. J. Denlinger, "A frequency dependent solution for microstrip transmission lines," *IEEE Trans. Microwave Theory Tech.*, vol. MTT-19, pp. 30–39, Jan. 1971.
[8] P. Silvester, "Skin effect in multiple and polyphase conductors," *IEEE Trans. Power Appl. Syst.*, vol. PAS-88, pp. 231–238, May 1969.
[9] Z. Csendes, A. Gopinath, and P. Silvester, "Generalised matrix inverse techniques for local approximations of operator equations," in *Mathematics of Finite Elements and its Applications*, J. Whiteman, Ed. New York: Academic, to be published.

Effect of Upper Sideband Impedance on a Lower Sideband Up-Converter

W. ALAN DAVIS AND PETER J. KHAN

***Abstract*—An analysis is given of a lower sideband up-converter which includes a finite circuit reactance X_{33} at the upper sideband frequency, in addition to the circuit impedances at the input signal and output lower sideband frequencies.**

The expressions developed for the gain, gain sensitivity to pump power variation, and noise figure show the extent to which gain and gain sensitivity decrease, and noise figure increases when X_{33} is finite, as compared to the case when X_{33} is infinite. For a simple circuit configuration the gain–bandwidth product changes markedly when X_{33} is small at the center frequency. In addition, when second-harmonic pump power is allowed to flow through the varactor diode, the performance of the lower sideband up-converter can be improved.

I. Introduction

THE lower sideband up-converter (LSUC) has been shown to have significant advantages over the reflection-type amplifier for low-noise receiver applications [1]. These advantages include a greater gain–bandwidth product, reduced gain sensitivity to pump power variations (at the expense of a very slight increase in noise figure and an output at an elevated frequency which limits input to low microwave frequencies), and elimination of the need for a circulator, which is also advantageous in cryogenic or miniaturized applications.

A significant problem in LSUC design has been the propagation of the upper sideband frequency; this is usually undesirable because power dissipation at this frequency in the diode and in the circuit resistances gives rise to degenerative feedback. A consequence is that the resulting induced positive resistance in the signal circuit subtracts from the parametrically generated negative resistance and reduces the gain.

Several authors have considered analytically the effect of upper sideband propagation in an LSUC. However, in most cases these authors have used a representation of the reverse-biased varactor-diode equivalent circuit consisting of a resistance and a variable capacitance in parallel [2], [3] or a lossless capacitance [4]. Although this simplifies the mathematics considerably, it yields significant inaccuracy when applied to multisideband circuits, since it leads to the erroneous conclusion that power dissipation in the diode can be avoided at harmonic sideband frequencies by the presence of a short circuit connected across the diode terminals. A more accurate approach, based upon matrix manipulation, has been used by Ernst [5] and by Howson and Smith [6], who carry out a general analysis of a multiple-sideband parametric network, using a diode representation consisting of a resistance in series with the variable capacitance. However, the work of Ernst is restricted to parametric amplifiers, while Howson and Smith consider only the multisideband converter having an output at the upper sideband frequency.

In most practical LSUC's, the upper sideband and the harmonic-sideband circuits consist of the diode series resistance R_s together with a reactance determined by the diode mount structure and the position of the pump, signal input, and lower sideband output filters. Loading of these sidebands with any resistance other than that resulting from the diode, transmission line, or filter losses is attainable only at the expense of considerable increase in circuit complexity.

This paper is concerned with the effect of upper sideband propagation on LSUC performance for the case where R_s is the only resistance in the upper sideband circuit. The study was motivated by the desire to answer the following two questions which arise in LSUC circuit design.

1) Over what range of values of the upper sideband circuit reactance X_{33} will the propagation of the upper sideband exert a negligible effect upon the operating performance of an LSUC which has been designed without considering the upper sideband?

2) Propagation of the upper sideband is known to provide a decrease in transducer power gain and in the gain sensitivity to pump power variations; this reduction in gain sensitivity is desirable for some applications. What is the extent of the increase in noise figure resulting from this upper sideband

Manuscript received August 21, 1972; revised January 29, 1973. This work was supported by the U. S. Army Electronics Command, Fort Monmouth, N. J., under Contract DAAB-07-68-C-0138.

W. A. Davis was with the Cooley Electronics Laboratory, Department of Electrical and Computer Engineering, University of Michigan, Ann Arbor, Mich. 48105. He is now with the Communications Research Laboratory, Department of Electrical Engineering, McMaster University, Hamilton, Ont., Canada.

P. J. Khan is with the Cooley Electronics Laboratory, Department of Electrical and Computer Engineering, University of Michigan, Ann Arbor, Mich. 48105.